

# EVALUATION OF A HIGH-POWER TARGET DESIGN FOR POSITRON PRODUCTION AT CEBAF\*

A. Ushakov<sup>1,2†</sup>, S. Covrig<sup>2</sup>, J. Grames<sup>2</sup>, S. Habet<sup>1,2</sup>, C. Le Galliard<sup>1</sup>, E. Voutier<sup>1</sup>

<sup>1</sup>Université Paris-Saclay, CNRS/IN2P3/IJCLab, Orsay, France

<sup>2</sup>Thomas Jefferson National Accelerator Facility, Newport News, USA

## Abstract

An injector for polarized positron beams at the Continuous Electron Beam Accelerator Facility (CEBAF) at Jefferson Lab is being designed. The Polarized Electrons for Polarized Positrons (PEPPo) concept is used to produce polarized  $e^+e^-$ -pairs from the bremsstrahlung radiation of a longitudinally polarized electron beam interacting within a high-Z conversion target. The scheme under consideration includes a 4 mm thick tungsten target that absorbs 17 kW deposited by a 1 mA continuous-wave electron beam with an energy of 120 MeV. The concept of a rotating tungsten rim mounted on a water-cooled copper disk was explored. The results of ANSYS thermal and mechanical analyses are discussed together with FLUKA evaluations of the radiation damages.

## INTRODUCTION

Positron beams (polarized and unpolarized) are an option for potential upgrades of CEBAF [1]. For many different types of electron scattering experiments, conducting the measurement with a positron beam will provide new experimental observables and will subsequently expand the physics reach of Jefferson Lab [2]. The PEPPo experiment [3] has demonstrated high efficiency of polarization transfer from electrons to the positrons through a two-step process: bremsstrahlung followed by pair production, with both reactions taking place (in series) in the same physical target. The polarization transfer is almost 100% at the high end of the positron energy spectrum. The positron polarization is proportional to the energy, but the number of highly polarized positrons is small and inversely proportional to the energy. Therefore, the quantity of interest, which characterizes a polarized source and further enters the statistical error of the measurement of experimental signals sensitive to the beam polarization, is the Figure-of-Merit (FoM) corresponding to the product of the beam intensity or current  $I$  with the square of the average longitudinal polarization  $\overline{P}_z$  of the beam population ( $\text{FoM} = I\overline{P}_z^2$ ). The FoM was used to optimize the target thickness and to select the positron energies [4] caught by the capture system of the polarized positron injector [5]. The essential differences between PEPPo and conventional unpolarized positron sources are using an initially polarized electron beam and selecting high-energy positron slices, an energy region featuring high polarization transfer [6, 7].

The repurposed Low Energy Recirculation Facility (LERF) is planned to be used for the generation, capture and acceleration of positron beams up to 123 MeV. A polarized electron source produces a continuous-wave (CW) high current ( $>1$  mA) and high polarization ( $>90\%$ ) beam, which is accelerated up to 120 MeV towards a high-power target for positron production. The optimal thickness of the tungsten target at 120 MeV is 4 mm [4]. A significant fraction of beam power is deposited in the target. The high non-uniform power deposition, quick temperature rise, mechanical stress and radiation damage could cause the target failure. The present work discusses a first evaluation of the possible parameters of the high-power target like the energy deposition, the level of radiation damage, and the expected temperature and mechanical stress.

## ENERGY DEPOSITION AND TARGET DESIGN

The energy deposition of the electron beam in the positron target was determined with FLUKA [8, 9]. The distribution of the energy deposited by a 120 MeV electron beam with a 1.5 mm RMS spot size in a stationary tungsten target of 4 mm thickness is shown in Fig. 1. The FLUKA data on the deposited energy was converted into power and imported as a heat source into ANSYS [10] to determine the temperature profile. For the 1 mA CW beam, the peak power density of  $324 \text{ W/mm}^3$  corresponds to  $324 \text{ MeV}/(e^- \cdot \text{mm}^3)$ .

To keep the temperature of the tungsten target at an acceptable level, the heat generated in the target by the beam must be distributed over a larger volume. The tungsten rim with a thickness of 4 mm is mounted on a water-cooled copper

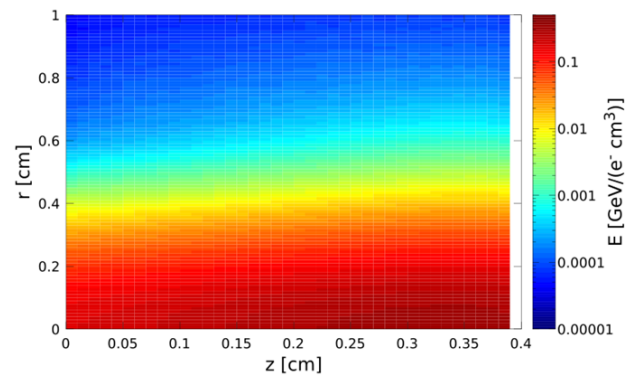


Figure 1: Energy deposition profile of a 120 MeV electron beam with a 1.5 mm RMS spot size in a 4 mm thick tungsten target.

\* This work was supported by the European Union's Horizon 2020 Research and Innovation program under Grant Agreement No 824093 and the U.S. DOE, Office of Science, Office of Nuclear Physics, contract DE-AC05-06OR23177.

† ushakov@jlab.org

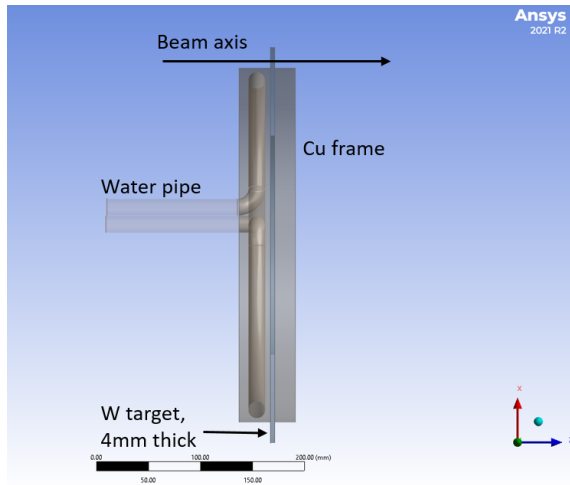


Figure 2: Conceptual design of the rotating target (side view).

disk. The side-view of the considered conceptual design of rotating target is shown in Fig. 2. The outer radius of the tungsten rim is 19 cm. The beam passes the target at a radius of 18 cm. The target rotation frequency considered in the temperature calculations was 2 Hz and the tangential speed of the beam moving on target was 2.3 m/s. The water channel inside the copper disk has a radius of 8 mm.

## TEMPERATURE AND STRESS CALCULATIONS

The full-time dependent CFD simulations were implemented. ANSYS Fluent has been used to calculate the temperatures in all parts of the target. The water flowing with a speed of 1.5 m/s (0.3 kg/s mass flow, 10 kPa pressure drop) was cooling the copper disk and tungsten rim mounted on the copper disk. For the 17 kW deposited in target beam power, the estimated maximal temperature of the water was about 30°C, and the peak temperature in the copper disk was below 100°C.

To simulate the heating of tungsten by the electron beam moving on the target, the distribution of heat power density was shifted by 0.56 mm along the circular path with a radius of 18 cm in 0.25 ms time steps (2.3 m/s). The heat distribution at one time step is shown in Fig. 3. For the selected point on target (at  $R = 18$  cm) and RMS beam size of 1.5 mm, the temperature rises during 4.5 ms and reaches the maximum of 681°C. Figure 4 shows the time evolution of temperature during the first 10ms of the 0.5s cycle (one complete turn of target). The spatial distribution of temperature is shown in Fig. 5.

The temperature distribution was imported into ANSYS static structural module to calculate the mechanical stress. Von Mises stress is a good measure of the proximity to failure of a material with values below material yield stress indicating an elastic behaviour [11]. Figure 6 shows the spatial distribution of equivalent von Mises stress. The maximal stress in tungsten is 878 MPa. Experimental testing of

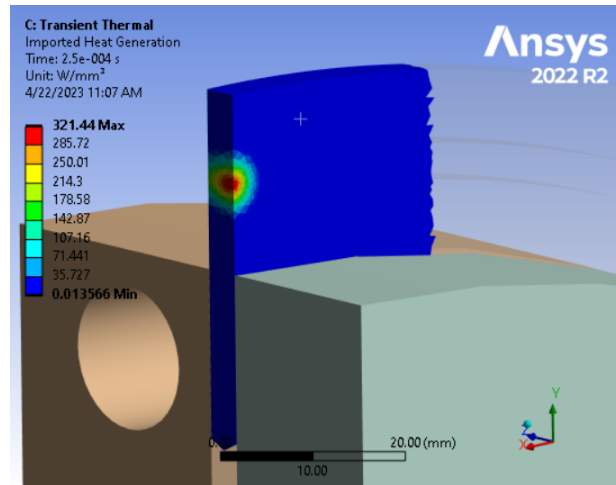


Figure 3: Distribution of heat power density of 1 mA electron beam at 120 MeV and 1.5 mm rms size in 4 mm thick tungsten.

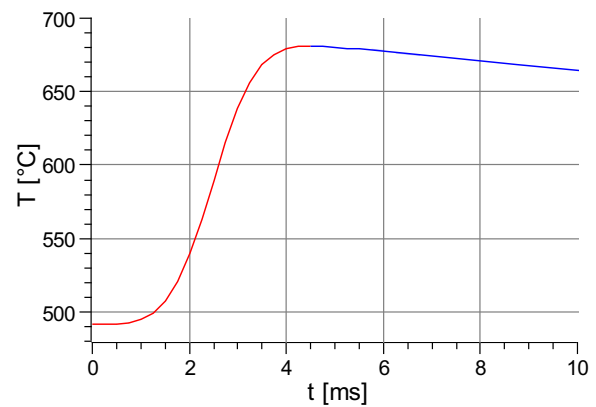


Figure 4: Cycling temperature in tungsten at radius of 18 cm rotated with the 2.3 m/s tangential velocity and 1.5 mm RMS beam spot (heating phase is shown in red and beginning cooling phase continued upto 0.5 s in blue).

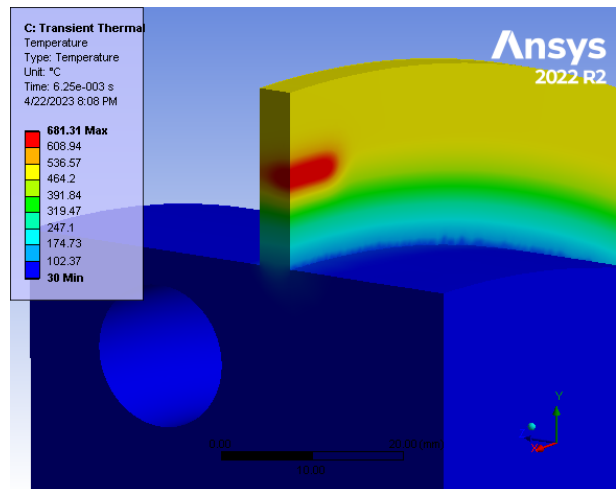


Figure 5: Temperature distribution in 17 kW target.

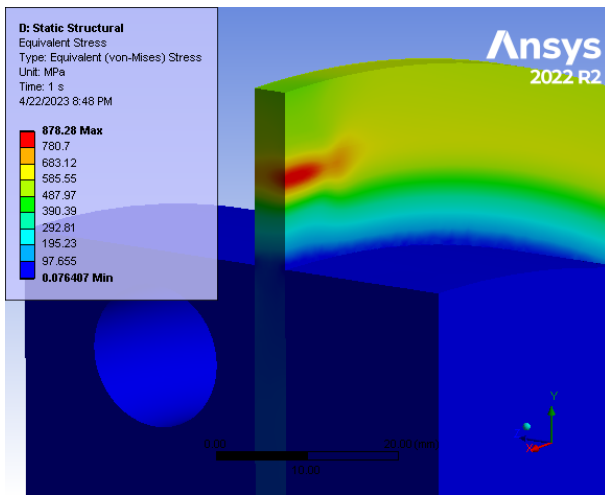


Figure 6: Mechanical stress induced by the temperature.

tungsten at these levels of mechanical stress and temperature is planned.

## RADIATION DAMAGE

FLUKA is used to determine the radiation damage of tungsten. Radiation damage effects are implemented in FLUKA for all particles, including recoils which have enough energy to induce damage to the materials [8]. The maximal damage is  $5.7 \cdot 10^{-22}$  displacements per atom (dpa) per  $e^-$ . Figure 7 shows the radiation damage at different depths of the spinning target with a diameter of 36 cm after 5000 h of irradiation. The calculated peak damage is 0.21 dpa. The effect of such radiation damage on material properties should be experimentally verified.

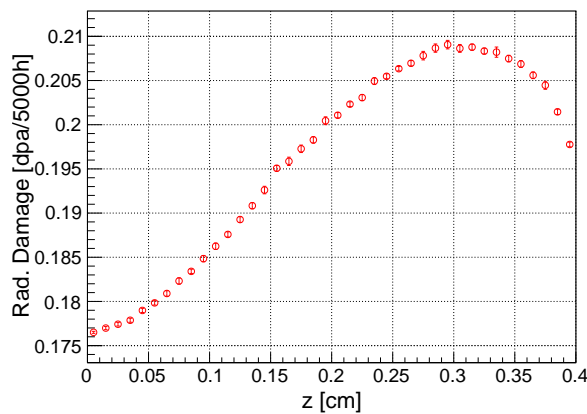


Figure 7: Radiation damage of W-target with  $\varnothing 36$  cm.

## OUTLOOK

A high-power target for positron production at the future  $Ce^+BAF$  positron injector [12] was evaluated. The full-time dependent CFD simulations (ANSYS Fluent) were implemented. The temperature, mechanical stress and radiation damage were calculated for the tungsten target with a thickness of 4 mm and 17 kW power deposited by 1 mA CW

electron beam with an energy of 120 MeV. The peak temperature of the target rotated with a velocity of 2.3 m/s is 680 °C and the maximal equivalent von Mises stress is 880 MPa. The estimated annual radiation damage is 0.21 dpa. To check if the target can be used safely extended period under such conditions and find experimentally the endurance stress limits and the impact of radiation damage on the material properties, the tests of the target materials (tungsten and tantalum) using 50  $\mu A$  at 3.5 MeV electron beam at Mainz Microtron (MAMI) have been started. Also, the material fatigue tests using the laser light are planned, similar to performed tungsten foil tests for APEX target at Jefferson Lab [13].

## REFERENCES

- [1] J. Arrington *et al.*, “Physics with CEBAF at 12 GeV and future opportunities,” *Progress in Particle and Nuclear Physics*, vol. 127, p. 103 985, 2022. doi: 10.1016/j.pnpnp.2022.103985
- [2] A. Accardi *et al.*, “An experimental program with high duty-cycle polarized and unpolarized positron beams at Jefferson Lab,” *The European Physical Journal A*, vol. 57, no. 8, 2021. doi: 10.1140/epja/s10050-021-00564-y
- [3] D. Abbott *et al.*, “Production of highly polarized positrons using polarized electrons at MeV energies,” *Phys. Rev. Lett.*, vol. 116, p. 214 801, 21 2016. doi: 10.1103/PhysRevLett.116.214801
- [4] S. Habet, A. Ushakov, and E. Voutier, “Characterization and optimization of polarized and unpolarized positron production,” Tech. Rep. JLAB-ACC-23-3794, 2023.
- [5] S. Habet *et al.*, “Concept of a polarized positron source for CEBAF,” in *Proc. IPAC’22, Bangkok, Thailand, 2022*, pp. 457–460. doi: 10.18429/JACoW-IPAC2022-MOPOTK012
- [6] H. Olsen and L. C. Maximon, “Photon and electron polarization in high-energy bremsstrahlung and pair production with screening,” *Phys. Rev.*, vol. 114, pp. 887–904, 1959. doi: 10.1103/PhysRev.114.887
- [7] E. A. Kuraev *et al.*, “Bremsstrahlung and pair production processes at low energies, multi-differential cross section and polarization phenomena,” *Phys. Rev. C*, vol. 81, p. 055 208, 2010. doi: 10.1103/PhysRevC.81.055208
- [8] C. Ahdida *et al.*, “New capabilities of the FLUKA multi-purpose code,” *Frontiers in Physics*, vol. 9, p. 788 253, 2022. doi: 10.1007/s11665-016-2457-x
- [9] G. Batistoni *et al.*, “Overview of the FLUKA code,” *Annals Nucl. Energy*, vol. 82, pp. 10–18, 2015. doi: 10.1016/j.anucene.2014.11.007
- [10] ANSYS. [www.ansys.com](http://www.ansys.com)
- [11] W. Stein *et al.*, “Thermal shock structural analyses of a positron target,” in *Proc. PAC’01, Chicago, IL, USA, 2001*, pp. 2111–2113. doi: 10.1109/pac.2001.987293
- [12] J. Games *et al.*, “Positron beams at  $Ce^+BAF$ ,” *To appear in these proceedings (MOPL152)*,
- [13] S. Gopinath and S. Covrig, “Hall A – APEX target thermal assesment,” Tech. Rep. PMAG0000-0001-A0001, 2020.